This document contains some information about an investigation on noise sensitivity of an Atomic Force Microscope.

It was written by Nils Schmeisser at Danish Institute of Fundamental Metrology.
You may not redistribute nor resale this document or parts of it.
If you use the document or parts of it you should place the folloing in your index section:

"AFM noise sensitivity", internal;
Nils Schmeisser, Danish Institute of Fundamental Metrology (DFM)

AFM noise sensitivity

Investigation on noise sensitivity of
Atomic Force Microscope (AFM)

Nils Schmeisser, February 1994

Introduction

It is well known that Atomic Force Microscopes (AFM) are sensitive to sound and vibration. To quantify this sensitivity data were recorded from an AFM in a controlled sound environment.
Using these data some qualitative and quantitative conclusions are done. Also some ideas how to prevent an AFM from such distortions are discussed.

AFM working principle

There are several imaging modes in the AFM. In the *Contact Mode*, which is described here, a sample is traced by a very thin tip which touches the surface with a mostly non-destructive force of about 10^{-7} to 10^{-10} N. While scanning over the surface relatively to a starting point a feedback system tries to keep the force constant by moving the sample away from or to the tip. This movement is recorded and reflects the relativ hight of a traced point compared to a base point. The spring constant k for a canteliver carrying the tip can be obtained with $k \leq 1$ N/m (ref. [1]) which is sufficient to get atomic resolution on the surface. The deflection of the spring (which is linear to the

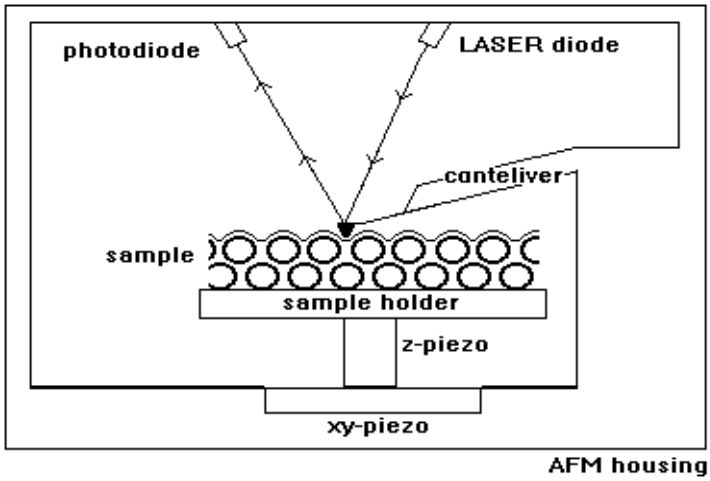

figure 1: The AFM setup. As the tip is mounted on a spring its vertical movement reflects a change of the force. The photodiode is a two segment photodiode and is therefore able to detect vertical movements of the tip. So the signal coming from the photodiode can be used to control the z-piezo, which moves the sample away from or to the tip in order to keep the force constant.

force working at the tip, $F=k*\Delta z$) is measured by a spring deflection sensor. Different kinds of these sensor are known. Only the optical sensor is described here because the AFM used in this investigation is based on this principle. Figure 1 shows the AFM working principle. The spring is typically made of silicon nitride (ref. [2]) and is covered with a reflecting gold layer.

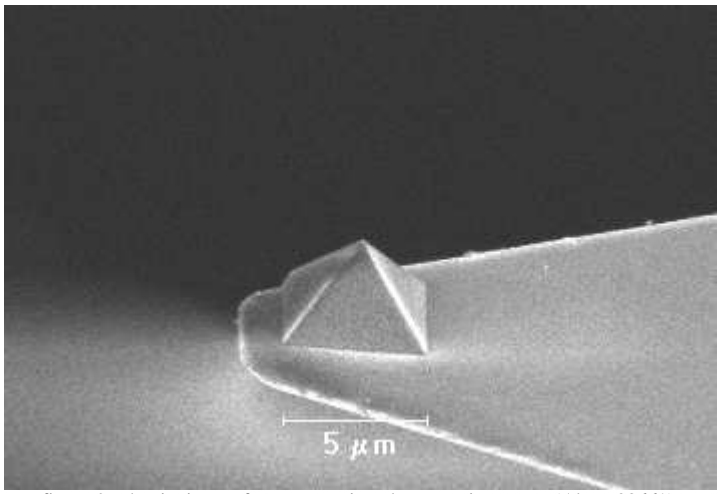

figure 2: The tip, image from a scanning electron microscope (5 kV, 3866*).

The Experiment

Experimental setup

The goal of the experiment was to find out how the AFM reacts on sound of certain frequencies. Therefore the first task for setting up the experiment was to prevent the system from uncontrolled external noise. A good way to do this was to hang up the AFM in a sound insulated chamber.

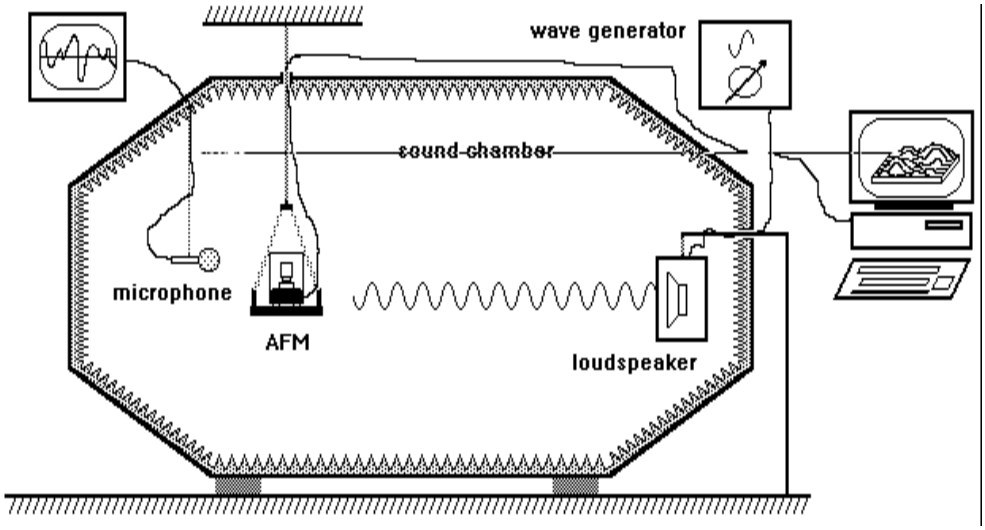

figure 3: Experimental setup. Both, the signal from the generator and the signal from the microphone had to be amplified.

The second task was to isolate the microscope from outside vibration. This was done by hanging it up by rubber bands which damp frequencies of approximately 5 Hz or higher. This is also the common way to place such a microscope in normal environment.
A loudspeaker and a microphone were inserted into the chamber where the loudspeaker was working as the sound source and the microphone as the sound sensor. The soundlevel representing the noise energy was measured as peak-to-peak voltage level of the amplified microphone signal and was then transformed to dB values by the formula *SL=U*maxdb/maxvolt+multdb* (ref. [3]) where *maxdb=60 dB, maxvolt=10 V* and *multdb=0 dB*. For the uncontrolled noise inside the chamber a 6 dB soundlevel was measured. The loudspeaker was connected via an amplifier to a signal generator which was able to produce sines waves with frequencies up to 20kHz.
During the experiment the force between the tip and the sample was measured via a headphone output which was integrated to the AFM. This output represented the loop controller error signal.
As sample material MICA (fig. 4) was chosen because of its well known regular surface structure which makes it easy to obtain information about distortions related to noise.

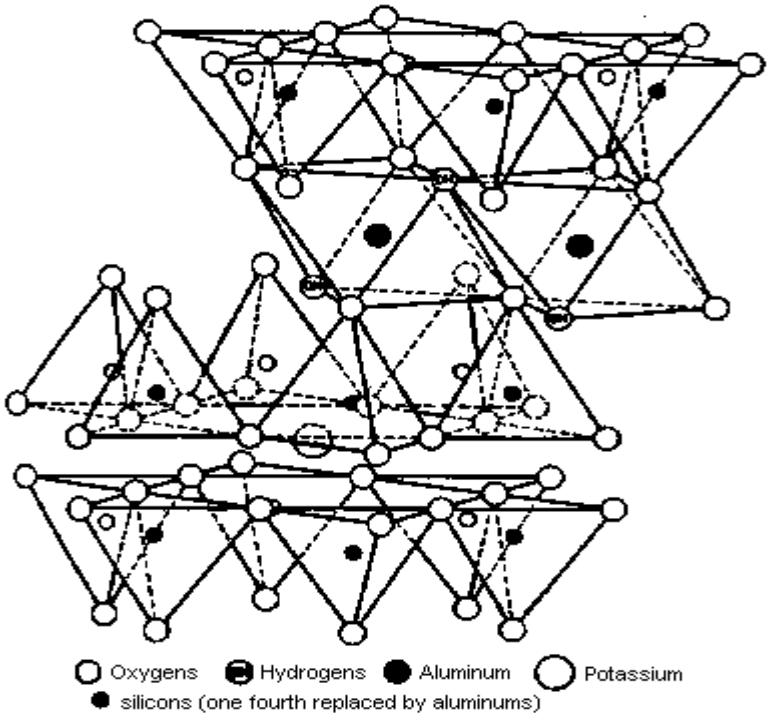

figure 4: Molecular structure of MICA

Proceeding the experiment

Def.: In the following a frequency f_R measured by the microphone is called resonance frequency of the microscope if the peak-to-peak level of the error signal as function of the sound frequency has a local maximum at f_R (assuming that the soundlevel is constant within a certain interval around f_R).

The experiment was performed in four steps:

1. **Seeking for resonance frequencies:**
   By tuning the frequency and the soundlevel local maximums of the error signal as function of the sound frequency where obtained.
2. **Constant Soundlevel:**
   Going through a frequency range up to 500 Hz and keeping the soundlevel at the microphone constant the peak-to-peak voltage of the error signal of the AFM loop controller was measured.
3. **Recording Response level:**
   While scanning under influence of sound of certain frequencies up to 1 kHz the soundlevel at each frequency was tuned until a minimal respond of the AFM was detected. Then the soundlevel was recorded.
4. **Measuring**
   a series of images of MICA influenced by sound signals within a frequency range up to 600 Hz. The images were stored for further investigation using DFM's image processing tools.

For step 4 a generator with frequency display was used. It was confirmed that the difference between the displayed frequency and the measured frequency was lower than the error rate of the frequency measurement. Therefore the frequency was directly obtained from the generator display.
Some remarks about error ranges are done in the Conclusion section.

In the next part the obtained data are presented by graphs and they will be shortly discussed.

1. Seeking for resonance frequencies

Starting with a low soundlevel the frequency was changed until a local maximum of the error signal was found. If within a certain frequency interval there was no maximum to be found the soundlevel was increased and the measurement started again for this interval. For high error signals the sound level was decreased to prevent the tip and the sample from damage.
Using this method within a search range from 0 Hz to 1.3 kHz nine resonance frequencies could be detected: 91.5, 141, 336, 505, 680, 861, 950, 1090 and 1230 Hz. They are shown as vertical lines in figure 5, 6 and 12.

2. Constant soundlevel

Holding a 24 dB soundlevel at the microphone for each frequency the data in table A.1 are obtained. The graph shows the error signal of the loop controller as function of the sound frequency. Two significant peaks, one around 110 Hz and the second around 325 Hz are observed. This allows the conclusion that the microscope is expected to have resonance frequencies close to these two frequencies.

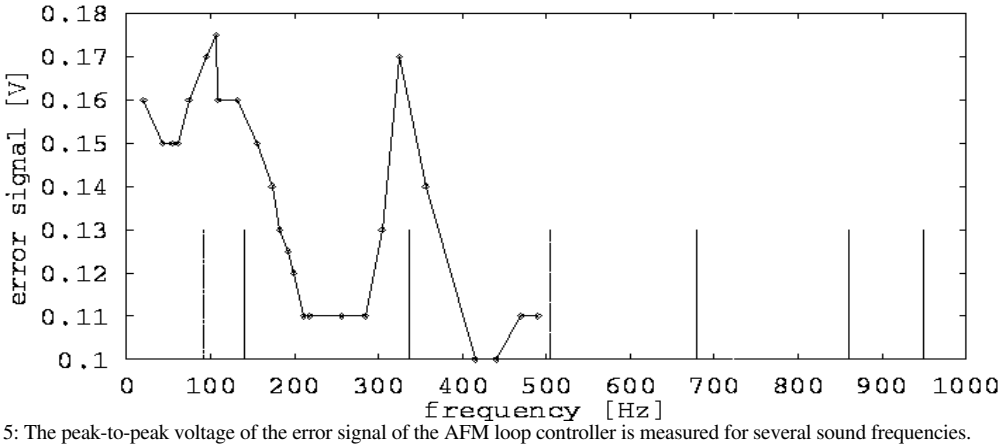

figure 5: The peak-to-peak voltage of the error signal of the AFM loop controller is measured for several sound frequencies.

3. Recording response level

The obtained data are documented in table A.2. The graph in figure 6 shows the sound level, which is necessary to make the microscope responding to a certain frequency. In this graph a low value means a high sensitivity of the microscope to noise.
90, 140, 195*, 230, 325*, 450, 650, 850 and 950 Hz are detected as frequencies with high response of the microscope (another description for a frequency to be a resonance frequency). The frequencies marked with stars are center values between neighboured frequencies with same response level.

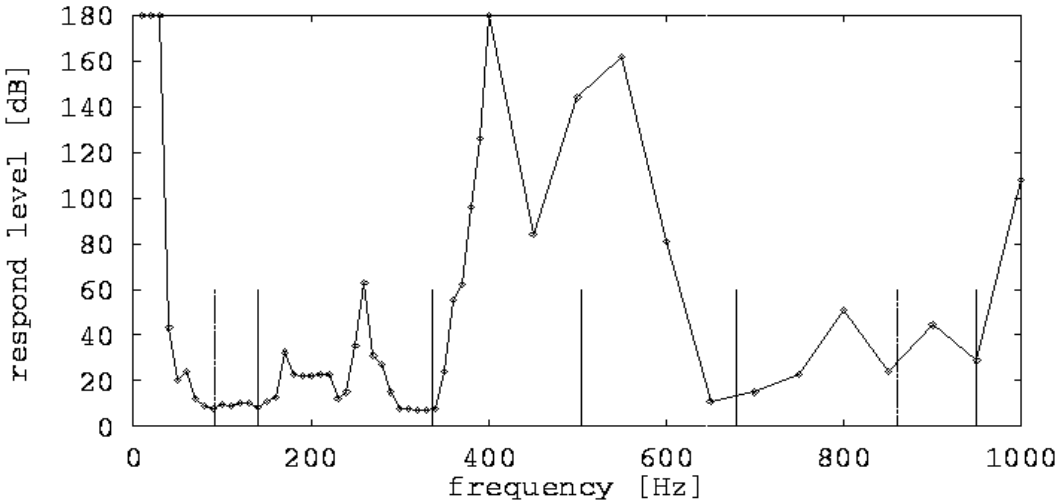

figure 6: The graph shows the minimal sound level where a reaction of the microscope could be detected.

This graph also shows that the microscope is most sensitive for frequencies within a range from about 50 Hz up to 500 Hz and from 600 Hz up to 1 kHz.

4. Scanning

Images influenced by sound were recorded over MICA with a range of 19.7*19.7 nm and a resolution of 256*256 pixel. The scanning speed was 430 nm/s and a force of 30 nN was used. In order to get good images at each sample point a pause of 5 µs was performed. The controller loopgain factor, giving the sensitivity of the feedback system was set to 0.2 which means a quite slow feedback (for higher loopgains the feedback system may become unstable).

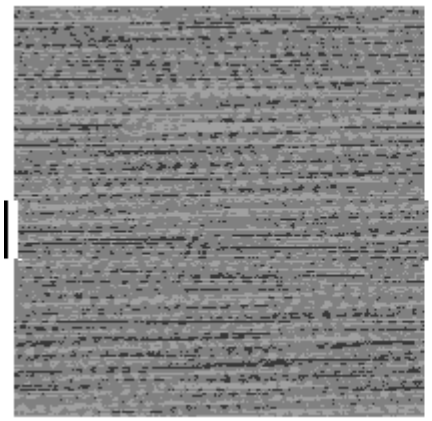

figure 7: MICA without sound

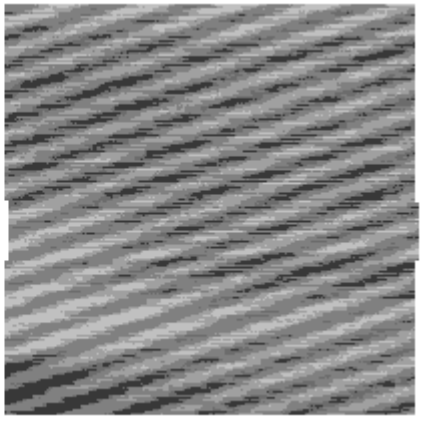

figure 8: MICA with 100 Hz sound

Figure 7 shows an image wihout sound influence and figure 8 an image taken with 100 Hz sound signal in the chamber. The sound can be detected and its frequency estimated from the Fourier transformed of the disturbed image, which is seen in figure 10.

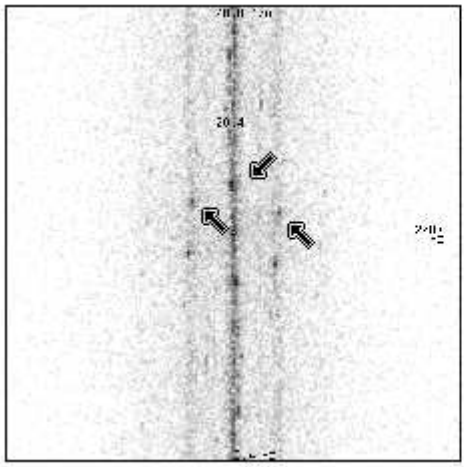

figure 9: Fourier transformation of fig. 7

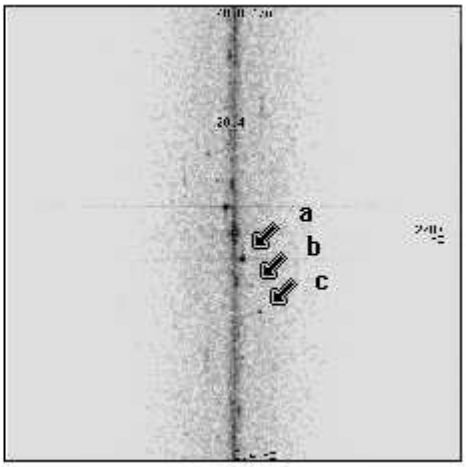

figure 10: Fourier transformation of fig. 8

Figure 9 shows the Fourier transformation of a sound free image. Here are the six peaks indicating the repeating structure of MICA clearly seen. The dark stripe along the y-axes might be due to 1/f noise from the building and/or from the electronics.
The Fourier transformation in figure 10 shows a case where the sound frequency was close to a resonance frequency. In this case it was impossible to detect any of the MICA peaks. Only the peaks for 100 Hz (a) its the second (b) and third harmonic (c) are seen. The time frequency f_n corresponding to a peak in the Fourier domain can be computed by

$$f_n=f_s*2*u/K$$

where f_s is the sampling frequency in x direction, u the frequency coordinate of the point and K the number of samples per line (ref. [4]). A peak is found by observing the image manually and computing the coordinates of a peak in an interval using an iterative sub-pixel search algorithm (the last part is done by a computer).
Figure 11 shows the detected sound frequencies as function of the sound frequencies in the chamber. It proofs the accuracy of detection of the sound signal by the way through the Fourier domain. Ideally the graph should follow the function $f(x)=\alpha*x$, where $\alpha=1$.

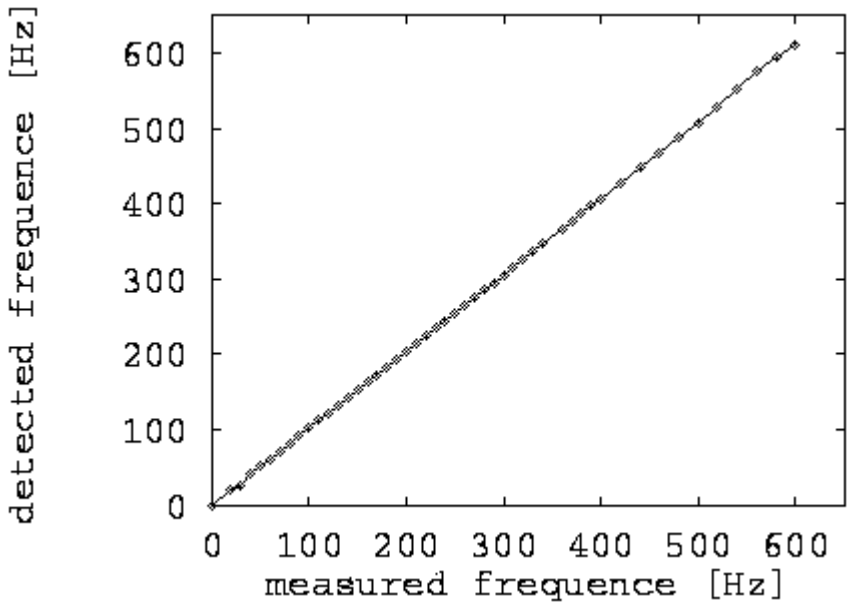

figure 11: Frequencies detected in the Fourier domain as function of measured frequencies

The statistical data analysis shows indeed that the relative difference between the ideal graph and the estimated on, defined as $\Delta f/f=(f_{Fourier}-f)/f$, is 2.37 % in mean with a standard deviation of 2.44 %. α is estimated as $\alpha=1.0237\pm0.0244$. Within an uncertainty range of 2.5 % for the frequency measurement this means that there is no significant difference between the frequency of the sound signal and its computed frequency.
Even resonance cases could be detected by recording the peak height of a certain frequency in the Fourier domain. The next diagram shows the computed peak levels of the detected sound peaks in the Fourier domain.

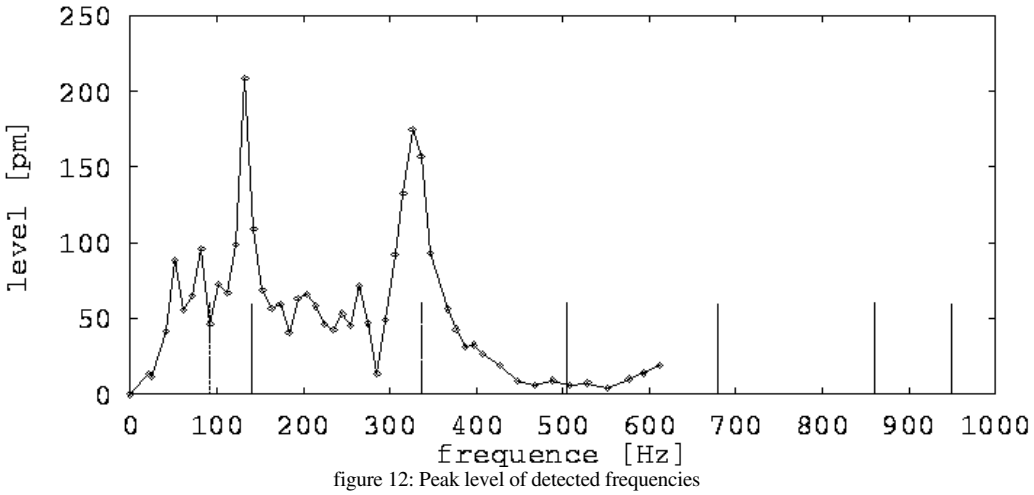

figure 12: Peak level of detected frequencies

Two significant peaks are seen. One at around 130 Hz the second around 320 Hz. These frequencies are close to the frequencies which were obtained from the earlier measurements. Also some less significant peaks are seen. For comparison, the peak values computed for the MICA peaks are only around 1.5 pm.

Results

The measurements were done by an oscilloscope and sometimes it was impossible to trigger the signals. The error range was estimated to 2.5 % for the frequency measurement and around 20 % for the voltage measurements. The error range was estimated from single measurements. Because the four measurements took place on different days, small differences of the obtained values are expected. Taking the error range into account the detected resonance frequencies are still significant. Therefore the following conclusions can be done:

1. It was possible to detect resonance frequencies of the AFM at 140 Hz and 325 Hz. There were also some less dominant frequencies.
2. This single microscope is most effected by frequencies between 50 Hz and 400 Hz and by frequencies between 600 Hz and 900 Hz. No conclusions can be done for the range above 1.2 kHz because there were no measurements.
3. Sound of a certain frequency could be detected by the use of the Fourier transformation. Figure 13 to 16 give an example how this information can be used to reconstruct a sound effected image. The peak corresponding to the 50 Hz sound is marked with an arrow, the MICA peaks are marked with circles.

fig. 13: MICA with 50 Hz (original)

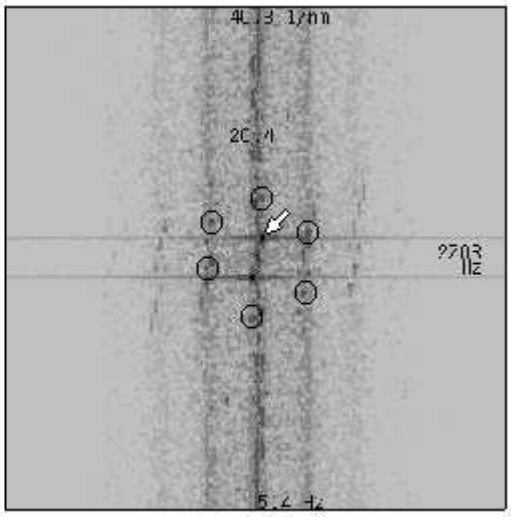

figure 14: Fourier transformation of fig. 13

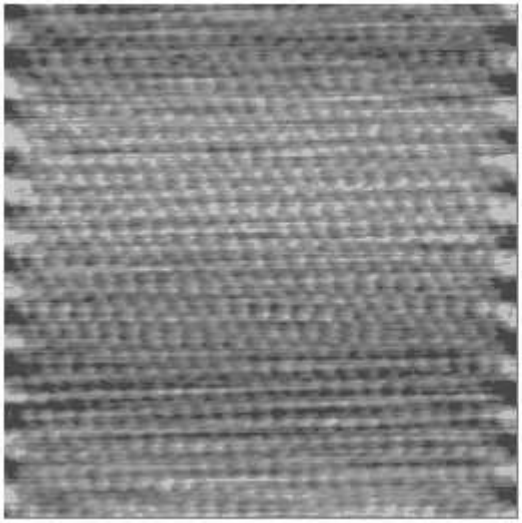

figure 15: inverse Fourier transformation of fig. 16

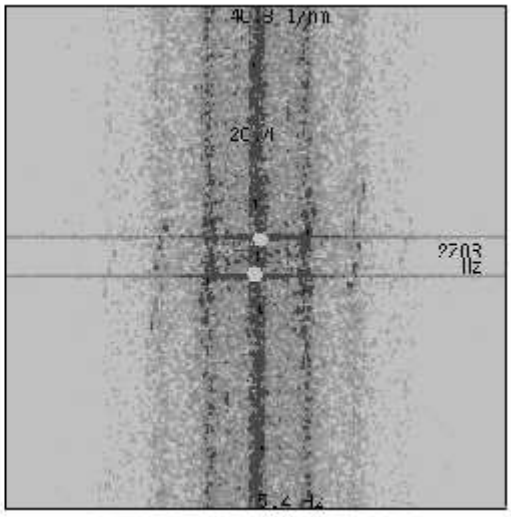

figure 16: fig. 14 with removed 50 Hz noise

The result looks quite good but because of 1/f sideband effects (The sidebands are seen in figure 16 as two parallel stripes surrounding

the 2703 Hz number.) and 1/f noise a full reconstruction was not possible.

These three conclusions allow to give a

Suggestion for placing an AFM

1. The AFM should be placed in a sound insulated box to prevent it from sound.
2. The eigenfrequencies of the placement should be higher than 1.2 kHz first not to effect the microscope and second because normal house noise/vibration is found in the range of 10 – 100 Hz (ref. [5]). The 1.2 kHz minimum eigenfrequency is estimated from the data of these experiments. Experiments covering a range over 1.2 kHz will return a more accurate suggestion about the minimum eigenfrequency.

To investigate on two simple placements the following computations are done.

AFM placed in 1-spring system

The AFM is placed in a sound insulated box (in the following called SIB) as it is shown in figure 17.

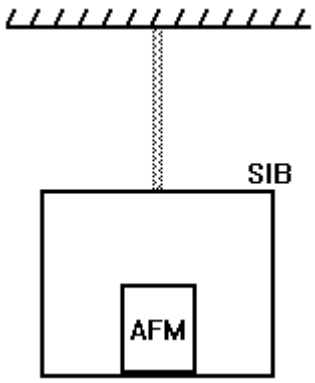

figure 17: AFM in 1-spring system

The equation of movement, taking a damping into account looks like

$$m \cdot \ddot{x} = -c \cdot x - k \cdot \dot{x} + P \cdot \sin(\omega \cdot t)$$

where c is the spring constant and k determines the damping factor. This leads to

$$x(t) = \frac{P \cdot \cos\varphi}{c - m\omega^2} \cdot \sin(\omega t - \varphi)$$

with

$$\tan\varphi = \frac{k\omega}{c - m\omega^2}$$

If $\cos\varphi$ is substituted by

$$\frac{1}{\sqrt{1 + \tan^2\varphi}}$$

the amplitude is given by the term

$$x_0 = \frac{P}{\sqrt{(c - m\omega^2)^2 + k^2\omega^2}}$$

The resonance frequency of the damped system can be obtained by

$$\omega_R = \sqrt{\frac{c}{m}}\sqrt{1 - \frac{k^2}{2mc}}$$

The following diagramm gives an overview on the reaction of the system to external vibration of frequency ω with respect to the damping k. k_k denotes the critical damping which is given by k_k=2*sqrt(c*m).

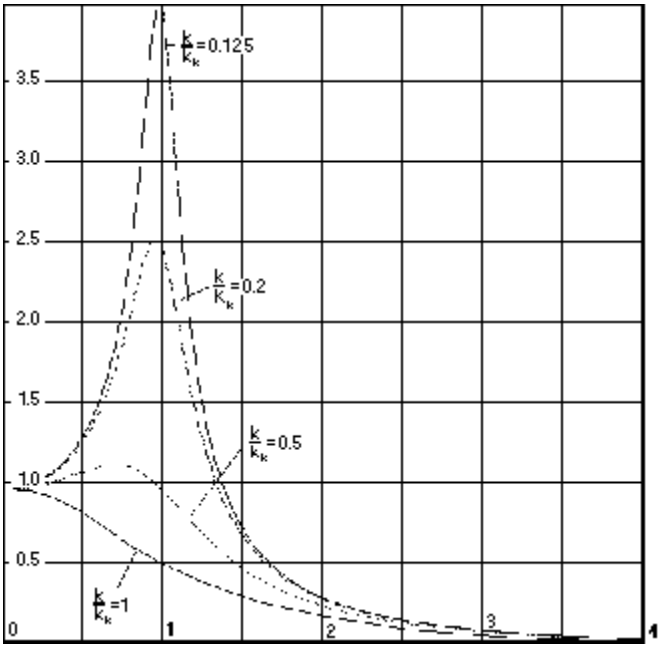

figure 18: system with one degree of freedom, the x-axes give the ratio w/sqrt(c/m), the y-axes displays the ratio amplitude of SIB to amplitude of distortion.

The eigenfrequency of

$$\omega_0 = \sqrt{\frac{c}{m} - \frac{k^2}{4m^2}}$$

allows to give a very important conlusion. If it is possible to tune the system to fullfill the condition

$$\frac{k^2}{4m^2} > \frac{c}{m}$$

the aperiodic case warranties the best damping for the system. Assuming a mass of the microscope of 50 kg (including the table) and c=218 N/m for the rubber bands used to hang up the microscopes at DFM the damping k should be higher than

k_k=2*sqrt(218 N/m*(50 kg + m_{SIB})).

The damping could be increased by the use of a high air resistive design of the SIB.

AFM placed in 2-spring system

Hanging up the AFM by rubber bands in the SIB too, the following configuartion should be discussed.

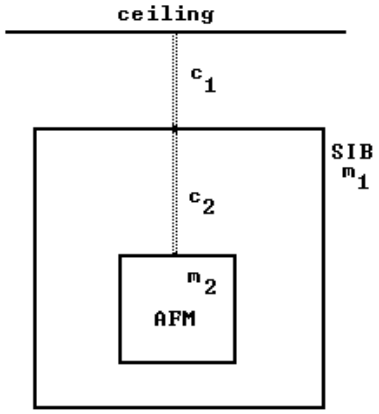

figure 19: AFM placed in 2-spring system

In this case the equation of movement looks like

$$m_1\ddot{x}_1 = -c_1x_1 + c_2(x_2 - x_1)$$
$$m_2\ddot{x}_2 = -c_2(x_2 - x_1)$$

if any damping is neglected. Assuming a distortion of

$$P(t) = P \cdot \cos(\omega t)$$

in the basement, the description of the system is given by

$$m_1\ddot{x}_1 = -c_1(x_1 - P \cdot \cos(\omega t)) + c_2(x_2 - x_1)$$
$$m_2\ddot{x}_2 = -c_2(x_2 - x_1)$$

Now, by substituting

$$\omega_1^2 := \frac{c_1 + c_2}{m_1},\ \omega_2^2 := \frac{c_2}{m_2},\ \omega_{10}^2 := \frac{c_1}{m_1} \text{ and } \mu := \frac{m_2}{m_1}$$

and using the differential operator

$$D = \frac{d}{dt}$$

the system can be transformed to

$$(D^2 + \omega_1^2)(D^2 + \omega_2^2)x_1 - \mu\omega_2^4 x_1 = \omega_{10}^2 P(D^2 + \omega_2^2) \cdot \cos(\omega t)$$

According to [6] the functions

$x_1(t)=A_1\cos(wt)$ and $x_2(t)=A_2\cos(wt)$

with

$$A_1 = \frac{\omega_{10}^2(\omega_2^2 - \omega^2)P}{(\omega_1^2 - \omega^2)(\omega_2^2 - \omega^2) - \mu\omega_2^4}$$

$$A_2 = \frac{\omega_{10}^2\omega_2^2 P}{(\omega_1^2 - \omega^2)(\omega_2^2 - \omega^2) - \mu\omega_2^4}$$

are solutions of the system. The situtation is shown in figure 20.

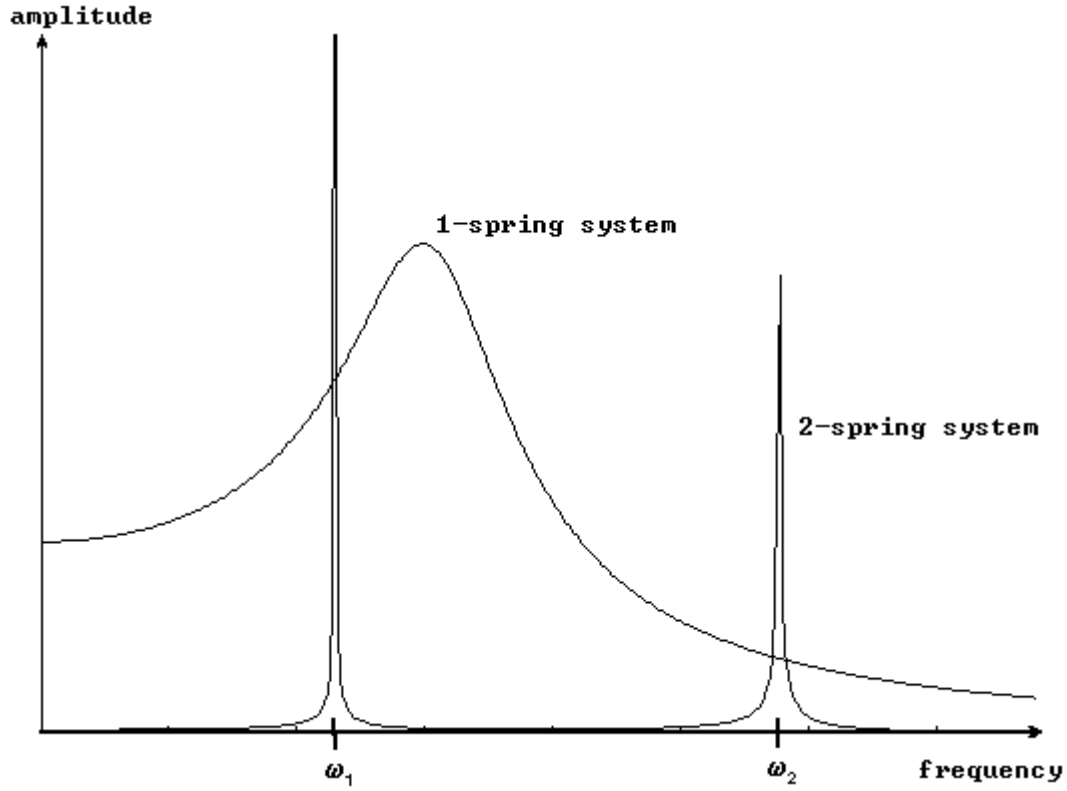

figure 20: Amplitude for the 1-spring and for the 2-spring case as function of the distortion frequency.

Comparing the two systems, the 2-spring system shows a disadvantage: there are two resonance frequencies. From this point it is strongly recommended to use as less as possible springs in the system in order to keep it controlable. A second effect which turns out is, that if

$$\omega = \omega_2 = \sqrt{\frac{c_2}{m_2}}$$

the amplitude A_1 of the SIB becomes 0, which means, that the SIB is undistorted by P*cos(w2t). But of course the AFM is still effected by the distortion. This effect offers a new possibility of damping the system, namely by using the 1-spring configuration but adding a spring c_D and a mass m_D at the bottom of the SIB to prevent the AFM from frequencies around sqrt(c_D/m_D). The only problem is how to control c_D or m_D to damp frequencies in a larger scale. Now, continuing with considering the 2-spring case, the next diagram shows, how the resonance frequencies are depent on the mass of the SIB.

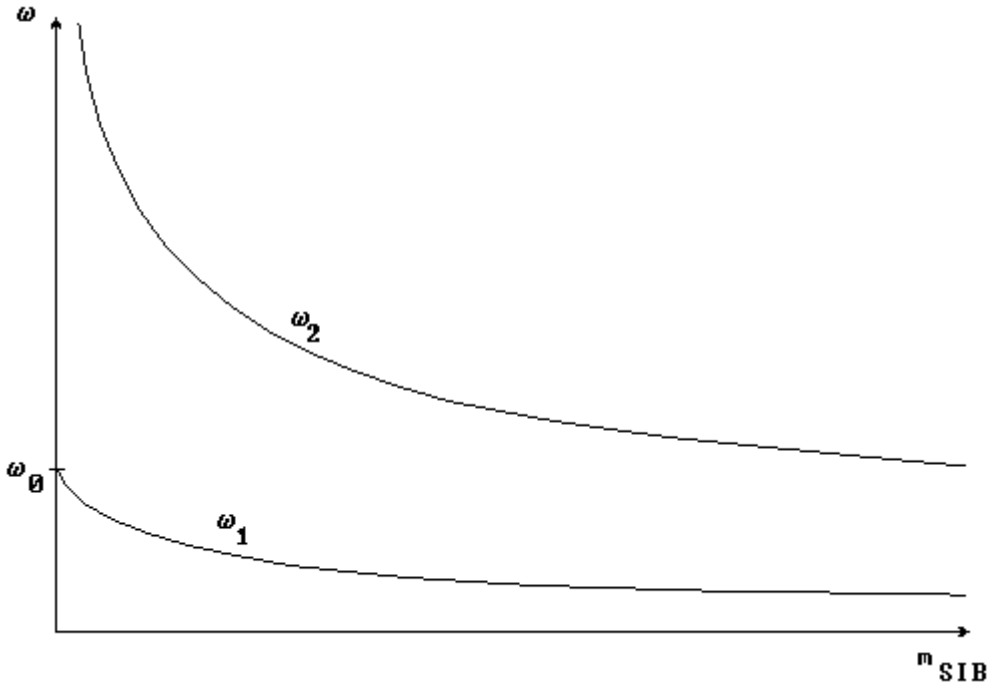

figure 21: Resonance frequencies as function of the mass of the SIB

Therefore it is possible to say that the properties of the system are as better as lighter the SIB is constructed.

Appendix A: Data

A.1 Constant soundlevel

Frequency [Hz]	Sound [V]	Soundlevel [dB]	Error signal [V]
20.0	3	18	0.16
43.0	4	24	0.15
54.0	4	24	0.15
60.5	4	24	0.15
74.0	4	24	0.16
94.5	4	24	0.17
107.0	4	24	0.175
109.0	4	24	0.16
132.0	4	24	0.16
155.0	4	24	0.15
173.0	4	24	0.14
182.0	4	24	0.13
192.0	4	24	0.125
198.6	4	24	0.12
211.0	4	24	0.11
218.0	4	24	0.11
256.0	4	24	0.11
284.0	4	24	0.11
304.0	4	24	0.13
324.4	4	24	0.17
356.0	4	24	0.14
415.0	4	24	0.10
440.0	4	24	0.10
470.0	4	24	0.11
490.0	4	24	0.11

A.2 Response level

Frequency [Hz]	Soundvoltage [V]	Soundlevel [dB]
10	-	-
20	-	-
30	-	-
40	7.2	43.2
50	3.4	20.4
60	4.0	24.0
70	2.0	12.0
80	1.5	9.0
90	1.3	7.8
100	1.6	9.6
110	1.5	9.0
120	1.7	10.2
130	1.7	10.2
140	1.4	8.4
150	1.8	10.8
160	2.1	12.6
170	5.4	32.4
180	3.8	22.8
190	3.7	22.2
200	3.7	22.2
210	3.8	22.8
220	3.8	22.8
230	2.0	12.0
240	2.5	15.0
250	5.9	35.4
260	10.5	63.0
270	5.2	31.2
280	4.5	27.0
290	2.5	15.0
300	1.3	7.8
310	1.3	7.8
320	1.2	7.2
330	1.2	7.2
340	1.3	7.8
350	4.0	24.0
360	9.2	55.2
370	10.4	62.4
380	16.0	96.0
390	21.0	126.0
400	-	-
450	14.0	84.0
500	24.0	144.0
550	27.0	162.0
600	13.5	81.0
650	1.8	10.8
700	2.5	15.0
750	3.8	22.8
800	8.5	51.0
850	4.0	24.0
900	7.4	44.4
950	4.8	28.8
1000	18.0	108.0

A.3 Measuring images

Series form Jan, 27th 1994

Parabolic Slope Correction

Image	Noise [Hz]	Level [V]	PK1 [pm]	PK2 [pm]	PK3 [pm]	N-freq [Hz]	Level [pm]
003	0	1.0	4.93808	0.00000	5.71400	0.000	0.0000
004	20	3.0	4.36912	1.23497	4.08226	21.190	13.2345

005	30	3.0	2.80021	0.00000	3.39545	24.500	11.8990	
006	40	3.6	5.93971	0.00000	4.20002	40.740	41.6185	
007	50	3.0	3.79025	0.00000	4.79664	51.550	88.2270	*
008	60	3.0	0.84216	0.00000	1.18996	61.120	55.4759	
009	70	3.0	0.00000	0.00000	0.00000	71.510	65.1398	
010	80	2.0	1.82148	0.00000	1.89183	82.230	95.7425	*
011	90	2.0	2.65017	0.00000	1.79592	92.210	46.6793	
012	100	2.2	0	0.00000	0.00000	101.860	72.7894	*
013	110	3.0	0	0	0	112.260	67.1271	
014	120	3.0	0.66141	0	0.67846	122.030	98.6319	
015	130	3.0	0	0	0	132.510	208.6210	*
016	140	3.0	0.49387	0	0.43999	142.740	109.2670	
017	150	3.0	0	0	0	152.730	68.6090	
018	160	2.8	0.65782	2.85522	1.17220	163.120	56.4561	
019	170	3.0	0.77349	0	0.83972	173.188	59.3364	*
020	180	3.0	0.75258	0	0.35736	183.337	40.7245	
021	190	2.8	0.47060	1.28629	1.22472	193.155	63.1751	
022	200	3.0	0.47368	0	0.31126	203.882	65.8078	*
023	210	3.0	0.76451	2.74269	1.10484	214.278	58.1224	
024	220	3.0	0.83175	3.23834	1.27694	224.014	46.3589	
025	230	3.0	0.66526	2.42116	1.32562	234.905	42.5861	
026	240	3.0	0.91598	3.07188	0.32621	244.972	53.2596	*
027	250	2.9	0.36146	0	0.75317	254.378	45.4359	
028	260	3.0	0.54141	2.97200	2.59661	264.526	71.2008	*
029	270	3.0	0.91556	2.75007	0.88210	274.675	46.8228	
030	280	3.0	0.03065	1.74418	0.30203	285.319	13.8451	
031	290	3.0	1.26879	4.33207	2.07538	295.138	49.3912	
032	300	3.0	0.68910	3.08202	0.75142	305.864	92.0917	
033	310	3.0	0.95436	3.03178	0.54217	315.600	132.2890	
034	320	3.0	1.31925	3.25930	1.06717	325.996	174.5640	*
035	330	3.0	0.88243	4.25655	0.24410	335.897	157.1410	
036	340	2.8	1.61887	2.57090	1.08010	346.376	93.4254	
038	360	3.0	0.47762	0	0.72122	366.509	56.2511	
039	370	2.8	1.08061	1.92082	1.18429	376.327	42.8830	
040	380	2.9	0.92896	3.93793	1.21534	387.301	31.3945	
041	390	3.2	0.88590	1.42848	1.66460	396.955	32.5958	*
042	400	3.0	1.06949	3.72726	1.88142	406.691	26.3078	
043	420	3.0	0.81849	2.13359	1.34016	427.483	19.1041	
044	440	3.0	0.47802	1.71546	2.14823	447.286	9.0665	
045	460	3.0	0.73380	0.85984	0.54392	467.418	5.9033	
046	480	3.0	0.69840	0	0.73298	488.376	9.0876	*
047	500	3.0	1.15504	3.35066	0.33124	508.178	5.7349	
048	520	3.0	1.11333	4.10351	0.39958	528.805	7.3452	
049	540	3.0	1.28956	2.18156	0.78224	551.578	4.3482	
050	560	3.0	0.97676	3.44283	0.57178	576.001	10.1207	
051	580	3.0	0.83606	1.78063	0.99631	593.823	13.9311	
052	600	3.0	0.78138	2.83167	0.75169	611.810	18.8779	

$d=\mathrm{Sum}((f_{mes}-f_{ind})/f_{ind})$ mean=2.37 %

std. dev.=2.44 %

Soundlevel SL [dB] = U*60 dB / 10 V+ 0dB

Appendix B: References

[1] Scanning Probe Microscopy; Investigation of Thin Organic Films; J. Garnaes; DFM-93-R4; pg. 6

[2] Artifacts in SPM; TopoMetrix Corporation; pg. 6

[3] Instructions and Applications for Microphone Amplifier Type 2603; Brueel & Kjaer; pg. 24

[4] Evaluation and Diagnosis of Scanning Probe Instruments by use of image processing (DFM-93-internal report); J.F. Joergensen, J. Garnaes, L. Nielsen;DFM; pg. 6

[5] STM and SFM in Biology; O. Marti, M. Amrein; Academic Press Inc.; pg. 66

[6] Gewoehnliche Differentialgleichungen; H. Heuser; B.G. Teubner Stuttgard; pg. 494